

PERFORMANCE OF THE DIGITAL LLRF SYSTEM AT THE cERL

F. Qiu[#], S. Michizono, T. Miura, H. Katagiri, D. Arakawa, T. Matsumoto, KEK, Ibaraki, Japan

Abstract

A digital low-level radio frequency (LLRF) system has been developed and evaluated at compact Energy Recovery Linac (cERL) in High Energy Accelerator Research Organization (KEK), Japan. A total of three two-cell cavities were installed for the injector, and two nine-cell cavities were installed for the main linac. The required RF stabilities for these cavities are 0.1% rms in amplitude and 0.1° rms in phase. To satisfy these requirements, we survey feedback parameters such as the proportional and integral (PI) gains. Furthermore, we evaluated the beam energy fluctuation due to the vector-sum controlling error between the cavities injectors 2 and 3. Finally, we present the performance of the LLRF system that was realized in the beam commissioning. This paper describes the current status of the LLRF system.

INTRODUCTION

The compact Energy Recovery Linac (cERL) is a prototype machine that was developed for the future next-generation light source accelerator 3-GeV ERL project, which is a superconducting project that is operated in continuous wave (CW) mode [1]. With cERL, a high accurate radio frequency (RF) field stability of 0.1% (in amplitude) and 0.1° (in phase) is required to achieve an excellent beam quality. For the future 3-GeV project, the RF field fluctuation should be maintained at less than 0.01% (in amplitude) and 0.01° (in phase). To realize such challenging RF field requirements, a μ TCA-based digital low-level RF (LLRF) system has been developed in the cERL.

To improve the performance of the LLRF system, the feedback gains such as the proportional and integral (PI) gains were optimized. Furthermore, we analyzed the effects of vector-sum control in the cavities of injectors 2 and 3. Finally, we summarize the performance of system.

This paper focuses on the current status and performance of the LLRF systems in the cERL. Optimization approaches and preliminary experiment results will also be presented.

LLRF SYSTEM

There is a total of six cavities in the cERL (see Table 1). All of them are superconducting cavities (SCs) with the exception of the buncher cavity, which is a normal conducting (NC) cavity. Both vector-sum control (for the cavity of injector 2&3) and individual cavity control (for the other cavities) are adopted in the cERL [2].

Figure 1 shows a schematic diagram of the LLRF system employed in the cERL. The 1.3-GHz cavity probe signal is down-converted to the 10-MHz intermediate frequency (IF) signal. The IF signal is sampled at 80 MHz

by a 16-bit ADC (LTC2208) and transmitted to a field-programmable gate array (FPGA). The base-band in-phase and quadrature (I/Q) components are extracted from the digitalized IF signal. After being filtered by a first order IIR low-pass filter, the I/Q components are regulated by a PI controller. The processed I/Q signal is fed into the I/Q modulator by a 16-bit DAC (AD9783) to re-generate the 1.3-GHz RF signal. Finally, the LLRF feedback loop is closed by driving a high power source to the cavities [3].

Table 1: Cavity Parameters

Cavity	Q_L	$f_{1/2}$ [Hz]	Ctrl. method
Buncher	1.125×10^4	57000	Individual ctrl.
Injector 1	1.2×10^6	540	Individual ctrl.
Injector 2	5.78×10^5	1120	Vector-sum control
Injector 3	4.8×10^5	1350	
ML1	1.3×10^7	50	Individual ctrl.
ML2	1.0×10^7	62	Individual ctrl.

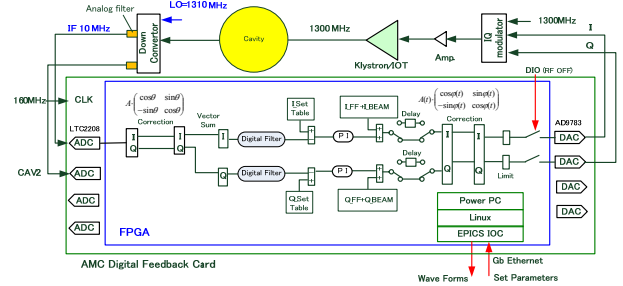


Figure 1: Schematic of the LLRF system in the cERL.

GAIN SCAN

To optimize the feedback gains in the PI controller (see Fig. 1) of the system, a gain scanning experiment was performed in the cERL. The system performance is measured, and recorded via different PI gains, and the optimal gains were determined according to the scanned performance curves. The detailed information about this scanning process was presented in [2] and [3].

Figure 2 shows the gain-scanning results obtained from the cavities of the buncher and injector 1. It should be noted that we normalized the gain in the digital PI controller to its analog form [2]:

$$K(z) = K_p + \frac{K_i}{1-z^{-1}} \Rightarrow K(s) = KP + \frac{KI}{s} \quad (1)$$

[#]qiufeng@post.kek.jp

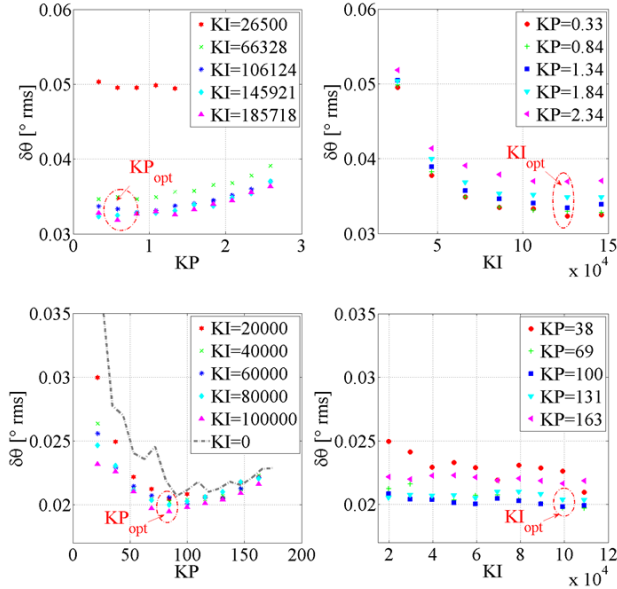


Figure 2: Gain scan results for the cavities of the buncher (upper) and injector 1 (lower). The optimal PI gains are indicated in the red circle.

In the lower figure of Fig. 2, we observe that, the proportional gain KP is the dominant gain. This conclusion can also be generalized to the other superconducting cavities. In the case of the NC cavity, such as the buncher cavity (upper figure in Fig. 2); a higher KP is not available because of its wider bandwidth; as a result, the integral gain KI is the dominant gain. Results for all of the six cavities are listed given in Table 2.

Table 2: Gain-scanning Results at the cERL

Cavity	KP_{opt}	KI_{opt}	Dominant Gain
Buncher	0.7	1.2×10^5	KI
Injector 1	84	1.0×10^5	KP
Injectors 2 and 3	41	1.1×10^5	KP
ML1	150	1.5×10^5	KP
ML2	150	1.5×10^5	KP

VECTOR -SUM CONTROL ANALYSIS

In a digital LLRF system, the true accelerating voltages (seen by the beam) are measured and calibrated by the digital board (FPGA and/or DSP). In practice, the voltages seen by the beam and the voltages measured by the digital LLRF system are not exactly the same (see Fig. 3). The difference (which can be expressed as a complex factor in Fig. 3) between them is the calibration error. These errors are usually insignificant for individual control. However, this situation is more complicated for the vector -sum control.

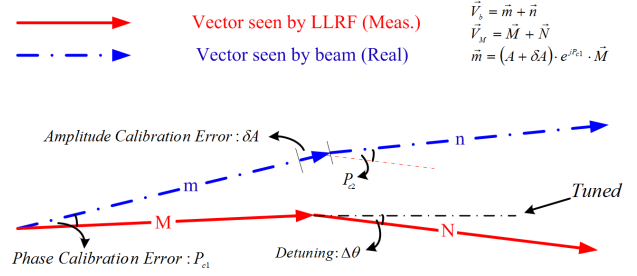


Figure 3: Vector-sum control with a phase/amplitude calibration error. The red lines (M and N) indicate the vector measured by the LLRF system, whereas the blue lines indicate the real vector seen by beam.

Owing to the existence of the calibration error, the detuning in the LLRF system (e.g., microphonics, power supply ripples, Lorentz detuning, etc.) will lead to a vector-sum error in the vector sum control. The phase calibration error in the system can be converted to an amplitude error in the vector-sum; conversely, the amplitude calibration error will lead to a phase error in the vector-sum. In the simplest vector-sum control in which one klystron drives two cavities (the same situation with the cavities of injectors 2 and 3 in cERL), the relation between the fixed phase calibration error and the vector-sum error in amplitude is given as

$$A_{vs} = \frac{P_{c1} - P_{c2}}{4} \cdot \sqrt{2} \Delta\theta = \frac{\Delta P_c}{4} \cdot \sqrt{2} \Delta\theta \quad (2)$$

where, the parameters P_{c1} and P_{c2} are the phase calibration errors of the first and second cavities, respectively. The parameter $\Delta\theta$ is the rms value of the detuning of each cavity. The cavities of injectors 2 and 3 are operated in the on-crest mode during the beam commissioning in the cERL (see Table 3), thus the amplitude error in the vector-sum is dominant, and therefore, we only consider the phase calibration error in this paper. The detailed discussion about vector-sum control is given in [4].

In the cERL, the difference in the calibrated phase for injectors 2 and 3 was mainly performed by a mechanical phase shifter that was installed in the line of injector 3 at the outside of the shield (see Fig. 4). We adjusted the phase shifter to increase the beam energy until the beam phase was on-crest in the cavities. The estimated deviation (ΔP_c) in the phase calibration in the adjustment is supposed to be 10° .

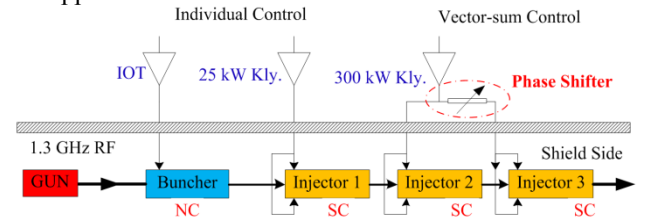


Figure 4: Layout of the injector cavities and RF system. The phase shifter is installed in the line of injector 3.

According to (2), the amplitude error in the vector-sum induced by detuning can be evaluated with the given

phase calibration error. In the cERL, the detuning of each cavity was regulated to approximately 1° (rms) by the tuner system. The measured detuning in injector 3 is shown in Fig. 5. As a result, an amplitude error of approximately 0.11% in the vector-sum can be calculated on the basis of (2). The cavities of injectors 2 and 3 will contribute about 7% of the total energy (~ 20 MeV); thus, the fluctuation in the beam momentum jitter induced by the amplitude error in the vector-sum is about 0.008% rms. This prediction was validated after we measured the beam momentum jitter during beam commissioning (see Fig. 6).

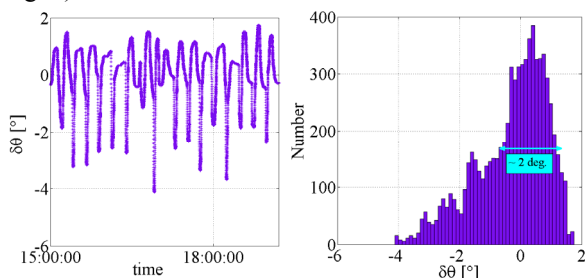


Figure 5: Detuning in the waveform (left) and histogram (right) of injector 3 cavities. The RMS value of the detuning is approximately 1° .

STABILITY

The typical LLRF system performance and operational parameters during beam commissioning are listed in Table 3. The feedback gains were determined by the gain-scanning experiments, as stated above. Disturbing signals such as microphonics and power supply ripples were suppressed well by the feedback [5]. Furthermore, the parasitic modes in the nine-cell cavities of the main linac were removed by a fourth order IIR filter [2]. The typical RF stabilities of the amplitude and phase, for the cavities in the main linac were, 0.012% and 0.015° , respectively, and for the cavities in the injector, they were 0.02% and 0.025° . All of them satisfied the requirements in cERL.

Table 3: Status of RF System in the Beam Commissioning

Cavity	ϕ_b	V_c	RF stability (RMS)	
			$\delta A/A$	$\delta\theta$
Buncher	-90°		0.05%	0.06°
Injector 1	0°	0.7 MV	0.02%	0.02°
Injector 2	0°	0.60 MV	0.02%	0.025°
Injector 3	0°	0.60 MV		
ML1	0°	8.56 MV	0.012%	0.014°
ML2	0°	8.56 MV	0.012%	0.015°

To measure the stability of beam energy, a screen monitor was installed downstream of the bending magnet with a 0.487-m dispersion, and a $63.7\text{-}\mu\text{m}/\text{pixel}$ resolution. The beam momentum jitter was then calculated by extracting the peak point information of the beam

projection in the screen monitor. The calculated beam momentum jitter was about 0.013% RMS as shown in Fig. 6. One of the possible reasons for the trend signal (indicated by the red line in the Fig. 6) in the beam jitter is the vector-sum error. This trend in the figure will contribute to an rms fluctuation approximately 0.01% of the total beam jitter. This result is in agreement with the previous analysis (0.008% rms).

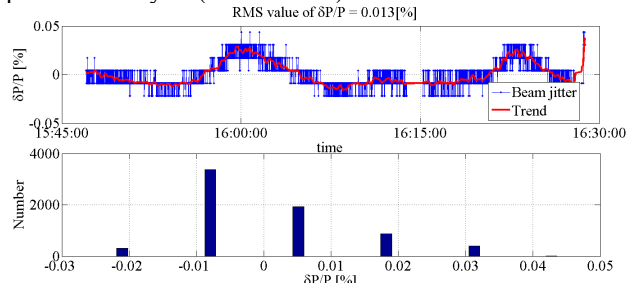


Figure 6: Beam momentum jitter. The measured beam momentum jitter was 0.013% rms, and the possible reason for the red line in the upper figure is the vector-sum error in the cavities of injector 2 and 3.

SUMMARY

Digital LLRF systems were installed for the injector and main linac in the cERL. To improve the performance of the LLRF systems, the feedback gains were surveyed and determined by performing a gain-scanning experiment. Furthermore, the vector-sum errors in the cavities of injectors 2 and 3 were analyzed and estimated. Finally, we summarized the performance of the LLRF system in the cERL, the typical RF stability values are 0.012% rms in amplitude and 0.015° RMS in phase for main linac cavities, and 0.02% rms in amplitude and 0.025° rms in phase for the injector cavities. This performance satisfied the required stability criteria of the cERL. Additionally, a beam momentum jitter of approximately 0.013% was achieved during beam commissioning.

REFERENCES

- [1] T. Miyajima, "Beam Commissioning of Energy Recovery Linacs", IPAC'13, Shanghai, May 2013, FRXBB201.
- [2] F. Qiu et al, "Feedback optimization in MicroTCA based LLRF system," RT2014, Nara, Japan, May, 2014.
- [3] F. Qiu et al., "Evaluation of the superconducting LLRF system at cERL in KEK", IPAC'13, Shanghai, May 2013.
- [4] A. Brandt, "Development of a Finite State Machine for the Automated Operation of the LLRF Control at FLASH," PhD thesis, DESY, 2007.
- [5] T. Miura et al., "Performance of RF System for Compact-ERL Main Linac at KEK", IPAC2014 Dresden, Germany.